Molecular Genetics and Metabolism xxx (2010) xxx–xxx

Contents lists available at ScienceDirect

Molecular Genetics and Metabolism

journal homepage: www.elsevier.com/locate/ymgme

Next generation sequencing in research and diagnostics of ocular birth defects

Gordana Raca [a,b,*], Craig Jackson [a], Berta Warman [d], Tom Bair [c], Lisa A. Schimmenti [d]

[a] *UW Cytogenetic Services, Wisconsin State Laboratory of Hygiene, 465 Henry Mall, Madison WI 53706, USA*
[b] *Department of Pathology and Laboratory Medicine, University of Wisconsin-Madison, 13000 University Avenue, Madison WI 53706, USA*
[c] *The University of Iowa DNA Facility, John W. Eckstein Medical Research Building, 431 Newton Rd, Iowa City, IA, USA*
[d] *Department of Pediatrics, Division of Genetics and Metabolism, University of Minnesota, 420 Delaware St. SE, Minneapolis, MN 55455, USA*

ARTICLE INFO

Article history:
Received 18 January 2010
Received in revised form 8 March 2010
Accepted 8 March 2010
Available online xxxx

Keywords:
Next generation sequencing
Sequence capture
GS FLX
Anophthalmia
Microphthalmia
Coloboma

ABSTRACT

Sequence capture enrichment (SCE) strategies and massively parallel next generation sequencing (NGS) are expected to increase the rate of gene discovery for genetically heterogeneous hereditary diseases, but at present, there are very few examples of successful application of these technologic advances in translational research and clinical testing. Our study assessed whether array based target enrichment followed by re-sequencing on the Roche Genome Sequencer FLX (GS FLX) system could be used for novel mutation identification in more than 1000 exons representing 100 candidate genes for ocular birth defects, and as a control, whether these methods could detect two known mutations in the *PAX2* gene. We assayed two samples with heterozygous sequence changes in *PAX2* that were previously identified by conventional Sanger sequencing. These changes were a c.527G > C (S176T) substitution and a single basepair deletion c.77delG. The nucleotide substitution c.527G > C was easily identified by NGS. A deletion of one base in a long polyG stretch (c.77delG) was not registered initially by the GS Reference Mapper, but was detected in repeated analysis using two different software packages. Different approaches were evaluated for distinguishing false positives (sequencing errors) and benign polymorphisms from potentially pathogenic sequence changes that require further follow-up. Although improvements will be necessary in accuracy, speed, ease of data analysis and cost, our study confirms that NGS can be used in research and diagnostic settings to screen for mutations in hundreds of loci in genetically heterogeneous human diseases.

Introduction

The goal of our study was to evaluate the capacity of array based sequence capture target enrichment (SCE) and massively parallel, next generation sequencing (NGS) to successfully identify mutations in candidate genes for the developmental ocular birth defects anophthalmia, microphthalmia and coloboma.

The advent of NGS technologies is expected to transform the practice of medical genetics [1–3]. With the high throughput and decreased sequencing costs achieved by NGS, it is no longer impossible to sequence hundreds or even thousands of exons and other genomic sequences in an individual with a suspected genetic disease. It is predicted that in the near future NGS might replace array based techniques and Sanger sequencing in their current clinical applications for the detection of mutations [1,3]. Additionally, NGS provides entirely new research and diagnostic capabilities, including whole genome screening for novel mutations and sequencing biological specimens for the genomic signature of novel infectious agents [4,5].

NGS could be particularly advantageous in research and testing for genetically heterogeneous hereditary conditions. Common disorders evaluated by clinical geneticists are caused by heterogeneous Mendelian loci and lend themselves to enrichment strategies followed by NGS. Examples include intellectual disability [6], deafness [7], familial cardiomyopathy [8] and retinitis pigmentosa [9]. In these conditions there are often very subtle phenotypic differences between affected patients to guide molecular diagnostics by indicating which gene is likely to be mutated in a particular individual. Current diagnostic evaluation proceeds by sequencing a series of genes, individually or in small sets, based on the relative frequency of the mutations and the sensitivity of available assays. If there is no predominant mutation(s) causing the disease, the pathogenic change often remains unknown even after very extensive and expensive molecular testing. With enrichment strategies followed by NGS, sequencing of all genes implicated in a particular genetic disorder could be performed simultaneously, efficiently and at low cost.

While clearly superior to traditional Sanger sequencing, NGS has had little impact on clinical testing to date. There are very few examples of successful application of NGS in translational research and diagnostics. Clinical testing using NGS is currently offered for Hypertrophic Cardiomyopathy (HCM), Dilated

[*] Corresponding author at: UW Cytogenetics Service, Wisconsin State Laboratory of Hygiene, 465 Henry Mall, Madison, WI 53706, USA. Fax: +1 608 265 7818.
E-mail address: racago@mail.slh.wisc.edu (G. Raca).

1096-7192/$ - see front matter © 2010 Elsevier Inc. All rights reserved.
doi:10.1016/j.ymgme.2010.03.004

Cardiomyopathy (DCM) and Long QT syndrome (http://www.genedx.com/). NGS has also been explored as a method to perform rapid human leukocyte antigen (HLA) typing for high resolution allele identification [10,11], and to develop assays for Neurofibromatosis Type 1 [12], autosomal recessive ataxia [13] and mitochondrial disorders caused by mutations in the mitochondrial genome and 362 nuclear genes controlling mitochondrial function [14]. Ng et al. applied targeted sequencing of all coding regions ("exome") to show the presence of causative mutations in four unrelated individuals with a rare dominantly inherited disorder, Freeman–Sheldon syndrome (FSS) [15] and to discover the gene for a rare recessive disorder of previously unknown cause, Miller disease [16]. Exciting applications have also been described in cancer research, where NGS has been applied in discovering new candidate genes for acute myeloid leukemia [17,18], glioblastoma multiforme [19] and other malignancies [20].

We describe the first study which showed the feasibility of using genomic enrichment by sequence capture followed by NGS to investigate genetic causes of the ocular birth defects anophthalmia, microphthalmia and coloboma. These eye anomalies are among the most prevalent causes of childhood blindness, affecting annually ~2 per 10,000 newborns worldwide [21]. Although they can be of different origins, the majority are caused by defects in genes which regulate normal eye development [22–25]. There is increased evidence that mutations in large numbers (possibly hundreds) of different genes can cause congenital eye malformations, but no single gene is responsible for a high percentage of cases [23–25]. Anophthalmia, microphthalmia and coloboma therefore represent disorders where simultaneous sequencing of large numbers of candidate genes by NGS is an ideal approach to study genetic causes and demonstrate the feasibility of NGS for clinical diagnostics.

We showed that the combination of array based SCE with resequencing on the GS FLX instrument using Titanium chemistry allows concurrent sequencing of more than 100 candidate genes for anophthalmia, microphthalmia and coloboma. However, improvements will be necessary in several areas including accuracy, speed, ease of data analysis and cost to allow successful diagnostic implementation of NGS for simultaneous mutation testing in hundreds of genes in genetically heterogeneous human diseases.

Materials and methods

We tested whether two known sequence changes in the renal-coloboma syndrome (a.k.a. Papillorenal syndrome, OMIM #120330) associated gene *PAX2*, which were previously characterized by Sanger sequencing, can reliably be detected by NGS. The first variant was a missense change in exon 5, c.527G > C, which resulted in serine to threonine amino-acid change S176T. This base substitution was identified in one of our previous studies in a father of a proband with ocular birth defects, but not in his affected child. Since detailed clinical information for the parent was not available, the change was described as a variant of unknown clinical significance.

Since short stretches of mono-, di-, and trinucleotide repeats represent hotspots for disease causing frameshift mutations in genomic DNA, we wanted to determine if this mutation type is detectable by NGS. Therefore, the second sequence change selected for the study was a deletion of one base in a polyG stretch in exon 2 of the *PAX2* gene (c.77delG), which has previously been described by Schimmenti et al. [26].

We designed a custom 385,000 probe SCE array with more than 100 candidate genes for eye malformations. The list of selected candidate genes is provided in Table 1. The genes were chosen based on reports of mutations identified in patients with coloboma, microphthalmia and anophthalmia [22,23,25]. Additionally, a comprehensive literature search was performed for published mutations associated with ocular phenotypes in animal models [27,28]. Some genes were included based on their role in signaling and developmental pathways which are known as important for eye formation and function [24].

Appropriate SCE probes for the regions of interest were chosen in collaboration with Roche-NimbleGen design team (Roche-NimbleGen, Madison, WI). Only protein coding regions (coding exons) of the 112 candidate genes were targeted on the array. We selected 385,000 long oligonucleotide probes (>60 bp) to tile the exons of the genes of interest with a very high density. All the probes had the uniqueness score of one (defined as having no match in the genome other than itself longer than 38 bp, allowing up to five insertions/deletions/mismatches in that match), to exclude repetitive regions from probe selection and avoid capturing pseudogene sequences [29]. Upon completion of the design and manufacturing of the array, the SCE on samples of genomic DNA from two patients with known mutations in the *PAX2* gene was performed at the NimbleGen service laboratory (Roche-NimbleGen, Madison, WI), following previously described protocols [30–32]. Briefly, ~20 µg of each patient's genomic DNA were randomly fragmented by nebulization to an average size of 500 bp. Linkers were ligated to the DNA fragments to provide a priming site for post-enrichment amplification of the eluted fragment pool. The fragments were denatured and hybridized to the custom SCE array. After a 72-h hybridization, unbound material was removed by stringent washing. The arrays were transferred to the NimbleGen elution system, and the enriched fragment pool was eluted and recovered from the array. The enriched fragments were amplified with 22mer linkers to generate enough DNA template for downstream applications. After amplification, the amount of captured DNA was measured by spectrophotometry and the product was tested for enrichment level by quantitative PCR with four proprietary QC control loci. These QC loci are conserved in both human and mouse genomes and have been empirically determined to accurately predict enrichment with several different array designs.

Sequencing of the two SCE prepared samples was performed on the GS FLX instrument using Titanium chemistry, at the University of Iowa DNA Facility following standard protocols. Two samples, separated by gaskets, were sequenced independently on two regions of the picotiter-plate. Briefly, amplified fragments from SCE were end-repaired and ligated to adapter oligonucleotides. The library was diluted based on the results of a previously performed titration, so that upon denaturation single DNA fragments hybridized to individual beads containing sequences complementary to adapter oligonucleotides. The beads were compartmentalized into water-in-oil microvesicles to allow clonal expansion of separate DNA molecules bound to the beads by emulsion PCR. After amplification, the emulsion was disrupted, and the beads containing clonally amplified template DNA were enriched. The beads were again separated by limiting dilution, deposited into individual picotiter-plate wells, and combined with sequencing enzymes. Iterative pyrosequencing was performed on the picotiter-plate by successive flow addition of the four dNTPs. A nucleotide-incorporation event in a well containing clonally amplified template produced pyrophosphate release and picotiter-plate well-localized luminescence, which recorded by a charge-coupled device (CCD) camera. With the flow of each dNTP reagent, wells were imaged, analyzed for their signal-to-noise ratio, filtered according to quality criteria, and subsequently algorithmically translated into a linear sequence output [33–35].

Data analysis was performed using the Roche proprietary software package for the GS FLX system. Image acquisition, image processing and signal processing were performed during the run. Post run analysis was conducted using the GS Reference Mapper.

Table 1
Candidate genes for anophthalmia, microphthalmia and coloboma represented on the SCE array.

Implicated in syndromic anophthalmia, microphthalmia and coloboma	Implicated in non-syndromic anophthalmia, microphthalmia and coloboma	Code for proteins on the SHH signaling pathway	Code for proteins on the WNT signaling pathway	Other
DPYD, SIX3, RAB3GAP, ZFHX1B, ALG3, PITX2, SHH, PTCH, POMT1, KIAA1279, RBP4, PAX2, PAX6, PTPN11, CREBBP, SALL1 NDP, MKS1, SALL4, PQBP1, BCOR, PORCN, IGBP1, FLNA, CHD7, CC2D2A, HMX1, CLDN19, LRP2, TFAP2A, IGBP1, IKBKG, B3GALTL, GDF6, SOX2,OTX2, JAG1, BMP4, MITF, HESX1	CHX10, MAF, SIX6, RAX	GLI2, GLI3, SMO,VAX1, VAX2, SUFU, DRM, CER1	DVL1, WNT1, WNT16, WNT5A, WNT5B, WNT7B, WNT7A, WNT2, WNT8A, WNT10A, WNT6, WNT8B, WNT3, WNT3A, WNT9A, WNT9B, WNT11, WNT4, WNT2B, LRP5, LRP6, FZD6, FZD9, FZD2, FZD1, FZD7, FZD5, FZD10, AXIN2, GSK3A, APC, CTNNB1	CRYAA, CRYAB, CRYBA1, CRYBA2, CRYBA4, CRYBB1, CRYBB2, CRYBB3, CRYGA, CRYGB, CRYGC, CRYGD, CRYGS, CRYZ SOX10, ZNF703, ZNF503 CRX, FOXG1,BMP7, CHD2, DLX1, DLX2, TBX2,TBX5, FGF8, HES1, LHX1
40 loci	4 loci	8 loci	32 loci	28 loci

Sequence runs were mapped against the human reference genome (hg18), using the default software settings (minimum base overlap of 40 bp and minimum overlap identity 90%). Sequence variations were detected automatically during mapping, and were annotated with known gene (refSeq genes from http://genome.ucsc.edu/) and SNP information (dbSNP129 from http://genome.ucsc.edu/). Variants were determined as high quality differences (HCDiffs) if the change was present in at least three non duplicate reads which included at least one read from each direction (forward and reverse). Additional analysis was performed with the CLC Genomic Workbench software (CLCbio, Aarhus, Denmark) and the NextGENe™ software (SoftGenetics, State College, PA).

Table 2
GS FLX sequencing summary.

	Sample 1	Sample 2
Sequence yield	214 Mb	191 Mb
Bases on target[a]	76.1 Mb	89.6 Mb
Average depth[b]	206	175.17
Average coverage[c]	99.24%	99.28%
% Covered ⩾15×	97.35	97.35
# Regions with <100% 15× coverage	54	54
# Regions without coverage	3	3
Total # of detected sequence changes	376	372
# Changes in coding regions	110	114
# Changes not corresponding to known SNPs	116	108
# Changes in coding regions not corresponding to known SNPs	26	26
# Changes likely to be real sequence alterations[d]	5	3

[a] Bases on target were determined based on rigorous criteria, so that bases that are a single-nucleotide outside of the captured region are not included in the count, even if they map to regions flanking the targets.

[b] Average depth is defined as average number of reads covering individual targeted nucleotides.

[c] Average coverage is the average proportion of bases within targeted exons which were covered by reads.

[d] These sequence variants met the following selection criteria: (1) they do not represent synonymous substitutions, (2) there is at least 30× coverage at the variant site and (3) the percentage of reads showing the variant allele exceeds 30%.

Results

We performed target enrichment by array based SCE and sequencing using GS FLX instrument on two DNA samples with known mutations in the *PAX2* gene. The sequencing was performed simultaneously for 112 candidate genes for ocular birth defects which were selected based on extensive literature search. A custom SCE array designed for target enrichment contained probes for all coding regions (total of 1017 exons) of the selected 112 genes. The size of the entire target region was 373,083 bp. Since 385,000 probe SCE arrays are able to capture up to 5 Mb of target sequence [32], our target region of ~0.37 Mb only used a portion of the capacity of the 385 K array. This allowed the use of a large number of probes per each targeted region and helped in obtaining good enrichment. DNA yield after elution from the SCE arrays and PCR amplification was approximately 10 µg for each sample; control loci showed 721-fold enrichment for the sample with the missense change (Sample 1), and 697-fold enrichment for the sample with the frameshift mutation (Sample 2).

The run on the GS FLX instrument using Titanium chemistry yielded 214 Mb of sequence for the first sample and 191 Mb for the second sample. Both met the Roche standard of at least 150 Mb per sample. 76.1 Mb of sequence mapped to the targeted regions for Sample 1, and 89.6 Mb for Sample 2 (Table 2); this proportion of bases on the target is comparable to what has previously been observed with array based SCE [12,15]. The average read lengths were 360 bp for Sample 1 and 318 bp for Sample 2. This is lower than the average read length for genomic samples but typical for samples prepared by SCE (The Roche standard is at least 300 bp). Details about the sequencing coverage obtained in the target regions are shown in Table 2 and in Fig. 1A and B.

For both samples, 94.7% of the captured regions showed ⩾15× coverage for all targeted bases (100%), with the average depth of coverage being ~206 for Sample 1 and ~175 for Sample 2. Only three regions showed complete lack of coverage. For 51 regions (out of a total of 1017) 15× coverage was not obtained for all the bases within a region. Most regions with low coverage (44/51) were identical between the two samples. The regions which completely lacked coverage were in both cases the first coding exons of the genes *WNT4*, *WNT9A* and *LRP5*, which were noted to have a very high GC-content (83%, 81% and 83%, respectively). Additionally, low complexity GC rich repetitive elements were present in the vicinity (100 bp upstream or downstream) of all the three exons without coverage. Unusual sequence characteristics with high GC-content and a presence of repetitive elements are well known causes of poor enrichment by SCE and decreased sequencing efficiency [12].

Studies have shown that the coverage in the 10–15-fold range may be sufficient for re-sequencing applications, but higher coverage depths (50–60-fold) provide better alignment, assembly and accuracy [36]. Therefore, most of our target exons have higher coverage than needed for a robust re-sequencing assay, allowing to expand our target region by incorporating additional genes and to sequence our samples as a pool.

The missense change in Sample 1 (c.527G > C, S176T) was easily identified by NGS. A total of 151 reads covered the variant site, with 52% of the reads showing the wild-type base and 48% showing the variant base, as would have been expected for a heterozygous allele. The c.527G > C change identified by Sanger sequencing is

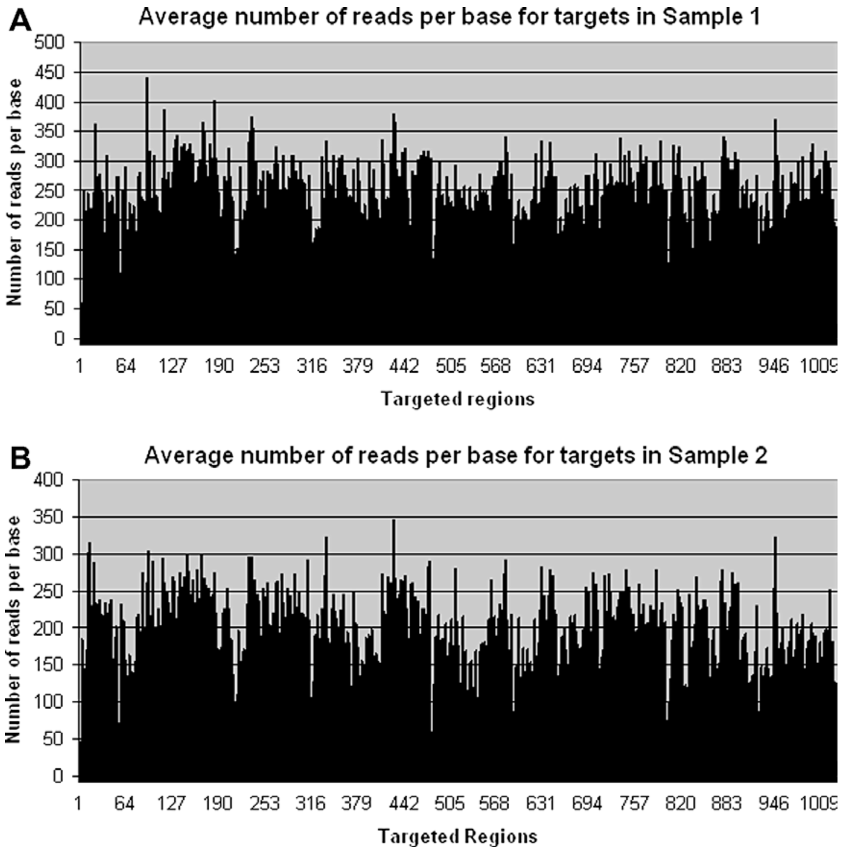

Fig. 1. (A and B) Average numbers of reads per base (depth of coverage) for each targeted region in Sample 1 (A) and Sample 2 (B). Although significant variation is noticeable between regions, sufficient coverage for reliable SNP detection was obtained for the majority of targeted exons.

shown in Fig. 2A, while the same change detected by NGS is presented in Fig. 2B.

A deletion of one base in a long polyG stretch was observed. A total of 76 reads covered the region, with $\sim$38% showing the wild-type allele (7 Gs), $\sim$54% showing the mutation (6 Gs) and the remaining $\sim$8% showing different numbers of Gs which did not correspond to either allele present in the sample (Fig. 3). Surprisingly, the c.77delG mutation was not registered by the GS Reference Mapper as a high quality difference. We therefore performed additional analysis with the CLC Genomic Workbench

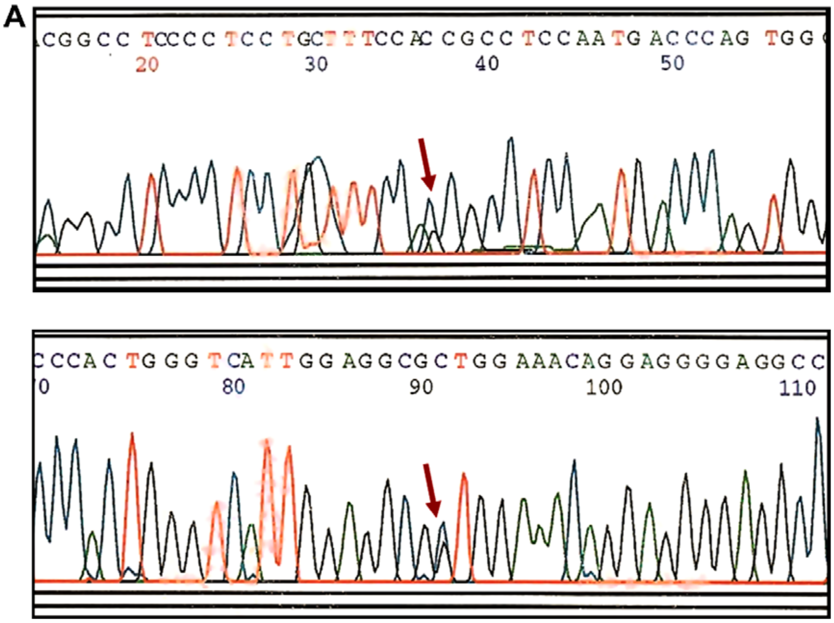

Fig. 2A. Sanger sequencing chromatograms showing the c.527G>C, S176T mutation in two different DNA strands. The mutated base is marked by the red arrow.

Please cite this article in press as: G. Raca et al., Next generation sequencing in research and diagnostics of ocular birth defects, Mol. Genet. Metab. (2010), doi:10.1016/j.ymgme.2010.03.004

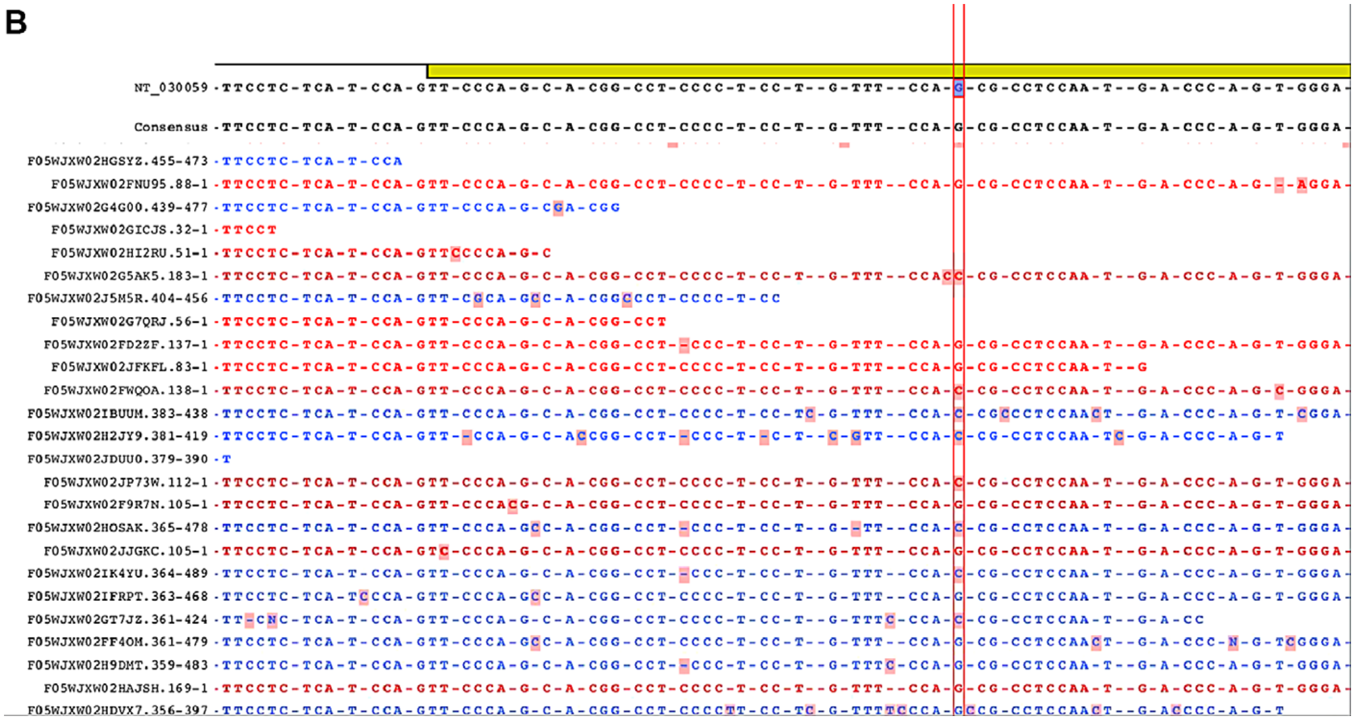

```
            NT_030059 -TTCCTC-TCA-T-CCA-GTT-CCCA-G-C-A-CGG-CCT-CCCC-T-CC-T--G-TTT--CCA-G-CG-CCTCCAA-T--G-A-CCC-A-G-T-GGGA-

            Consensus -TTCCTC-TCA-T-CCA-GTT-CCCA-G-C-A-CGG-CCT-CCCC-T-CC-T--G-TTT--CCA-G-CG-CCTCCAA-T--G-A-CCC-A-G-T-GGGA-
F05WJXW02HGSYZ.455-473 -TTCCTC-TCA-T-CCA
   F05WJXW02FNU95.88-1 -TTCCTC-TCA-T-CCA-GTT-CCCA-G-C-A-CGG-CCT-CCCC-T-CC-T--G-TTT--CCA-G-CG-CCTCCAA-T--G-A-CCC-A-G---AGGA-
F05WJXW02G4G00.439-477 -TTCCTC-TCA-T-CCA-GTT-CCCA-G-CGA-CGG
   F05WJXW02GICJS.32-1 -TTCCT
   F05WJXW02HI2RU.51-1 -TTCCTC-TCA-T-CCA-GTTCCCCA-G-C
  F05WJXW02G5AK5.183-1 -TTCCTC-TCA-T-CCA-GTT-CCCA-G-C-A-CGG-CCT-CCCC-T-CC-T--G-TTT--CCACC-CG-CCTCCAA-T--G-A-CCC-A-G-T-GGGA-
F05WJXW02J5M5R.404-456 -TTCCTC-TCA-T-CCA-GTT-CGCA-GCC-A-CGGCCCT-CCCC-T-CC
   F05WJXW02G7QRJ.56-1 -TTCCTC-TCA-T-CCA-GTT-CCCA-G-C-A-CGG-CCT
  F05WJXW02FD2ZF.137-1 -TTCCTC-TCA-T-CCA-GTT-CCCA-G-C-A-CGG-CCT--CCC-T-CC-T--G-TTT--CCA-G-CG-CCTCCAA-T--G-A-CCC-A-G-T-GGGA-
   F05WJXW02JFKFL.83-1 -TTCCTC-TCA-T-CCA-GTT-CCCA-G-C-A-CGG-CCT-CCCC-T-CC-T--G-TTT--CCA-G-CG-CCTCCAA-T--G
  F05WJXW02FWQOA.138-1 -TTCCTC-TCA-T-CCA-GTT-CCCA-G-C-A-CGG-CCT-CCCC-T-CC-T--G-TTT--CCA-C-CG-CCTCCAA-T--G-A-CCC-A-G-C-GGGA-
F05WJXW02IBUUM.383-438 -TTCCTC-TCA-T-CCA-GTT-CCCA-G-C-A-CGG-CCT-CCCC-T-CC-TC-G-TTT--CCA-C-CGCCCTCCAACT--G-A-CCC-A-G-T-CGGA-
F05WJXW02H2JY9.381-419 -TTCCTC-TCA-T-CCA-GTT--CCA-G-C-ACCGG-CCT--CCC-T--C-T--C-GTT--CCA-C-CG-CCTCCAA-TC-G-A-CCC-A-G-T
F05WJXW02JDUU0.379-390 -T
  F05WJXW02JP73W.112-1 -TTCCTC-TCA-T-CCA-GTT-CCCA-G-C-A-CGG-CCT-CCCC-T-CC-T--G-TTT--CCA-C-CG-CCTCCAA-T--G-A-CCC-A-G-T-GGGA-
  F05WJXW02F9R7N.105-1 -TTCCTC-TCA-T-CCA-GTT-CCCACG-C-A-CGG-CCT-CCCC-T-CC-T--G-TTT--CCA-G-CG-CCTCCAA-T--G-A-CCC-A-G-T-GGGA-
F05WJXW02HOSAK.365-478 -TTCCTC-TCA-T-CCA-GTT-CCCA-GCC-A-CGG-CCT--CCC-T-CC-T--G--TT--CCA-C-CG-CCTCCAA-T--G-A-CCC-A-G-T-GGGA-
  F05WJXW02JJGKC.105-1 -TTCCTC-TCA-T-CCA-GTC-CCCA-G-C-A-CGG-CCT-CCCC-T-CC-T--G-TTT--CCA-G-CG-CCTCCAA-T--G-A-CCC-A-G-T-GGGA-
F05WJXW02IK4YU.364-489 -TTCCTC-TCA-T-CCA-GTT-CCCA-G-C-A-CGG-CCT--CCC-T-CC-T--G-TTT--CCA-C-CG-CCTCCAA-T--G-A-CCC-A-G-T-GGGA-
F05WJXW02IFRPT.363-468 -TTCCTC-TCA-TCCCA-GTT-CCCA-GCC-A-CGG-CCT-CCCC-T-CC-T--G-TTT--CCA-G-CG-CCTCCAA-T--G-A-CCC-A-G-T-GGGA-
F05WJXW02GT7JZ.361-424 -TT-CNC-TCA-T-CCA-GTT-CCCA-G-C-A-CGG-CCT-CCCC-T-CC-T--G-TTTC-CCA-C-CG-CCTCCAA-T--G-A-CC
F05WJXW02FF4OM.361-479 -TTCCTC-TCA-T-CCA-GTT-CCCA-GCC-A-CGG-CCT-CCCC-T-CC-T--G-TTT--CCA-G-CG-CCTCCAACT--G-A-CCC-N-G-TCGGGA-
F05WJXW02H9DMT.359-483 -TTCCTC-TCA-T-CCA-GTT-CCCA-G-C-A-CGG-CCT--CCC-T-CC-T--G-TTTC-CCA-G-CG-CCTCCAA-T--G-A-CCC-A-G-T-GGGA-
  F05WJXW02HAJSH.169-1 -TTCCTC-TCA-T-CCA-GTT-CCCA-G-C-A-CGG-CCT-CCCC-T-CC-T--G-TTT--CCA-G-CG-CCTCCAA-T--G-A-CCC-A-G-T-GGGA-
F05WJXW02HDVX7.356-397 -TTCCTC-TCA-T-CCA-GTT-CCCA-G-C-A-CGG-CCT-CCCCTT-CC-TC-G-TTTTCCCA-GCCG-CCTCCAACT--G-ACCCC-A-G-T
```

Fig. 2B. A screenshot from the CLCbio analysis software showing the missense mutation c.527G>C, S176T. Reads from different directions are shown in different colors (red and blue). The mutated base is shown between the two vertical red lines.

and the NextGENe™ analysis programs, focusing only on sequence changes in the coding region of the *PAX2* gene. The c.77delG was clearly identified both by the CLC Genomic Workbench and the NextGENe™ analysis. Reasons for the discrepancy between different analysis tools are unclear, however, it is well known that pyrosequencing based methods (like GS FLX) tend to erroneously interpret long stretches (>6) of the same nucleotide [33,37]. To compensate for the resulting "noise" at all homonucleotide sites the GS Reference Mapper may be less likely to register base deletions and insertions at such regions.

We performed detailed analysis of sequence changes detected in targeted genes other than *PAX2*, to determine how well can SCE–NGS be applied to analysis of unknown samples from patients with eye anomalies. Since NGS applications usually identify a large amount of genetic variation, we wanted to determine if false positive findings (sequencing errors) and benign polymorphisms can readily be distinguished from possibly pathogenic changes which require further follow-up. The summary of this analysis is provided in Table 2. To consider clinically important variants, both in the SCE array design and in the analysis, we focused only on coding sequences. Both homozygous and heterozygous changes were included, since both recessive and dominant models of inheritance are considered for the studied disorders. We filtered out all known nonpathogenic single-nucleotide polymorphisms reported in the dbSNP database (http://www.ncbi.nlm.nih.gov/projects/SNP/). This left the total of 26 changes in coding regions not corresponding to known SNPs in both Sample 1 and Sample 2 (Table 2). We than applied three additional previously described parameters to further reduce the number of candidate mutations in tested samples. We focused only on changes detected in the regions with sufficient coverage (>30×) with the rationale that those are less likely to represent false positives [36]. We also eliminated synonymous base changes, which did not result in amino-acid changes. Knowing that the samples were sequenced individually and that mosaicism for point mutations is very rare in patients with genetic disorders, we also required that the percentage of reads showing the variant allele exceeds 30% [12]. Using these filters we reduced the number of detected coding alterations which were likely to represent real sequence changes (rather than sequencing errors) to five (two frameshift and three missense mutations) in Sample 1 and three (two frameshift and one missense mutation) in Sample 2 (listed in Table 3). Only these eight alterations were selected for confirmation by Sanger sequencing, although the presence of other real sequence changes (which did not meet our selection criteria) could not be excluded. The base substitutions (missense mutations) detected by NGS were also identified by Sanger sequencing, but the frameshift mutations were not confirmed (Table 3). This is not surprising, however, since all the frameshift mutations detected by NGS (deletion "CGA" in the *FGFR2* gene, deletion "T" in the *CHD2* gene, deletion "A" in the *APC* gene and deletion "A" in the *LRP2* gene) mapped to long homonucleotide stretches, where sequencing errors are known to occur with GS FLX technology. Although the frameshift changes listed in Table 3 meet stringent selection criteria, they still represent false positives, showing the difficulty in accurate detection of frameshift mutations by pyrosequencing based NGS technologies.

PolyPhen (http://genetics.bwh.harvard.edu/pph/) and SIFT (http://sift.jcvi.org/) analyses were performed to examine the likelihood that the observed missense changes alter the functions of the encoded proteins. Both analysis tools predicted one missense mutation (R942C in the RAB3GAP1 protein) to be probably damaging, and one (I744 V in ZEB2) to be likely benign (Table 3). However, for the remaining two amino-acid changes (I3389 V in LRP2 and L1129S in APC) PolyPhen and SIFT gave different predictions, thus showing that an accurate determination of functional significance of amino-acid changes in proteins cannot be achieved based solely on computer analysis. In summary, although confirmation by Sanger sequencing and the use of bioinformatics tools may have decreased the number of sequence variants which would have needed further studies in unknown samples, our

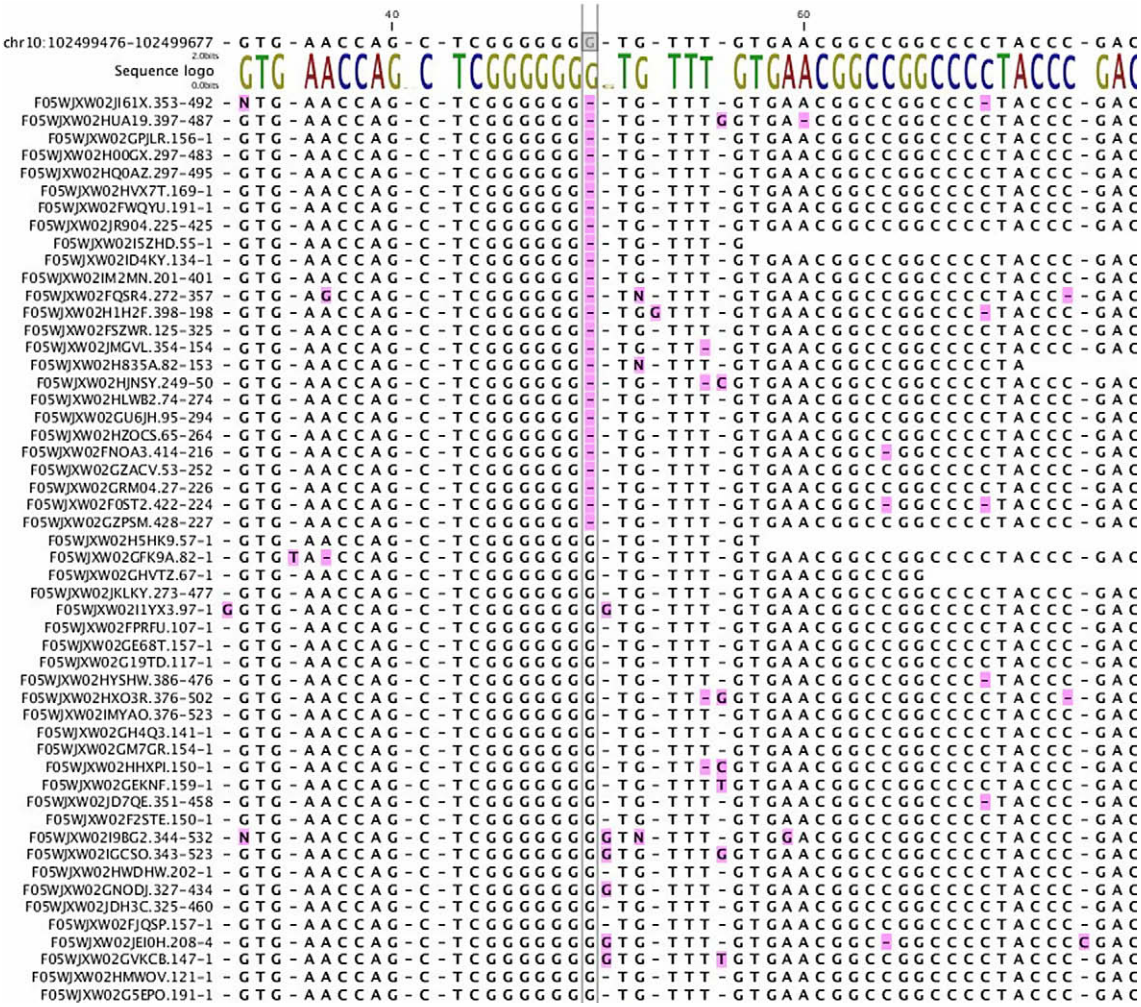

```
                                     40                      60
                                     |                       |
chr10:102499476-102499677 -GTG-AACCAG-C-TCGGGGGGG-TG-TTT-GTGAACGGCCGGCCCCTACCC-GAC
                  2.0bits
            Sequence logo  GTG AACCAG C TCGGGGGGG TG TTT GTGAACGGCCGGCCCcTACCC GAC
                  0.0bits
   F05WJXW02JI61X.353-492 -NTG-AACCAG-C-TCGGGGGG--TG-TTT-GTGAACGGCCGGCCC-TACCC-GAC
   F05WJXW02HUA19.397-487 -GTG-AACCAG-C-TCGGGGGG--TG-TTTGGTGA-CGGCCGGCCCCTACCC-GAC
     F05WJXW02GPJLR.156-1 -GTG-AACCAG-C-TCGGGGGG--TG-TTT-GTGAACGGCCGGCCCCTACCC-GAC
   F05WJXW02H00GX.297-483 -GTG-AACCAG-C-TCGGGGGG--TG-TTT-GTGAACGGCCGGCCCCTACCC-GAC
   F05WJXW02HQ0AZ.297-495 -GTG-AACCAG-C-TCGGGGGG--TG-TTT-GTGAACGGCCGGCCCCTACCC-GAC
     F05WJXW02HVX7T.169-1 -GTG-AACCAG-C-TCGGGGGG--TG-TTT-GTGAACGGCCGGCCCCTACCC-GAC
     F05WJXW02FWQYU.191-1 -GTG-AACCAG-C-TCGGGGGG--TG-TTT-GTGAACGGCCGGCCCCTACCC-GAC
   F05WJXW02JR904.225-425 -GTG-AACCAG-C-TCGGGGGG--TG-TTT-GTGAACGGCCGGCCCCTACCC-GAC
      F05WJXW02ISZHD.55-1 -GTG-AACCAG-C-TCGGGGGG--TG-TTT-G
     F05WJXW02ID4KY.134-1 -GTG-AACCAG-C-TCGGGGGG--TG-TTT-GTGAACGGCCGGCCCCTACCC-GAC
   F05WJXW02IM2MN.201-401 -GTG-AACCAG-C-TCGGGGGG--TG-TTT-GTGAACGGCCGGCCCCTACCC-GAC
   F05WJXW02FQSR4.272-357 -GTG-AGCCAG-C-TCGGGGGG--TN-TTT-GTGAACGGCCGGCCCCTACC--GAC
   F05WJXW02H1H2F.398-198 -GTG-AACCAG-C-TCGGGGGG--TGGTTT-GTGAACGGCCGGCCC-TACCC-GAC
   F05WJXW02FSZWR.125-325 -GTG-AACCAG-C-TCGGGGGG--TG-TTT-GTGAACGGCCGGCCCCTACCC-GAC
   F05WJXW02JMGVL.354-154 -GTG-AACCAG-C-TCGGGGGG--TG-TT--GTGAACGGCCGGCCCCTACCC-GAC
    F05WJXW02H835A.82-153 -GTG-AACCAG-C-TCGGGGGG--TN-TTT-GTGAACGGCCGGCCCCTA
    F05WJXW02HJNSY.249-50 -GTG-AACCAG-C-TCGGGGGG--TG-TT-CGTGAACGGCCGGCCCCTACCC-GAC
    F05WJXW02HLWB2.74-274 -GTG-AACCAG-C-TCGGGGGG--TG-TTT-GTGAACGGCCGGCCCCTACCC-GAC
    F05WJXW02GU6JH.95-294 -GTG-AACCAG-C-TCGGGGGG--TG-TTT-GTGAACGGCCGGCCCCTACCC-GAC
    F05WJXW02HZOCS.65-264 -GTG-AACCAG-C-TCGGGGGG--TG-TTT-GTGAACGGCCGGCCCCTACCC-GAC
   F05WJXW02FNOA3.414-216 -GTG-AACCAG-C-TCGGGGGG--TG-TTT-GTGAACGGC-GGCCCCTACCC-GAC
    F05WJXW02GZACV.53-252 -GTG-AACCAG-C-TCGGGGGG--TG-TTT-GTGAACGGCCGGCCCCTACCC-GAC
    F05WJXW02GRM04.27-226 -GTG-AACCAG-C-TCGGGGGG--TG-TTT-GTGAACGGCCGGCCCCTACCC-GAC
   F05WJXW02F0ST2.422-224 -GTG-AACCAG-C-TCGGGGGG--TG-TTT-GTGAACGGC-GGCCC-TACCC-GAC
   F05WJXW02GZPSM.428-227 -GTG-AACCAG-C-TCGGGGGG--TG-TTT-GTGAACGGCCGGCCCCTACCC-GAC
      F05WJXW02H5HK9.57-1 -GTG-AACCAG-C-TCGGGGGGG-TG-TTT-GT
      F05WJXW02GFK9A.82-1 -GTGTA-CCAG-C-TCGGGGGGG-TG-TTT-GTGAACGGCCGGCCCCTACCC-GAC
      F05WJXW02GHVTZ.67-1 -GTG-AACCAG-C-TCGGGGGGG-TG-TTT-GTGAACGGCCGG
   F05WJXW02JKLKY.273-477 -GTG-AACCAG-C-TCGGGGGGG-TG-TTT-GTGAACGGCCGGCCCCTACCC-GAC
      F05WJXW02I1YX3.97-1 GGTG-AACCAG-C-TCGGGGGGGGTG-TTT-GTGAACGGCCGGCCCCTACCC-GAC
     F05WJXW02FPRFU.107-1 -GTG-AACCAG-C-TCGGGGGGG-TG-TTT-GTGAACGGCCGGCCCCTACCC-GAC
     F05WJXW02GE68T.157-1 -GTG-AACCAG-C-TCGGGGGGG-TG-TTT-GTGAACGGCCGGCCCCTACCC-GAC
     F05WJXW02G19TD.117-1 -GTG-AACCAG-C-TCGGGGGGG-TG-TTT-GTGAACGGCCGGCCCCTACCC-GAC
   F05WJXW02HYSHW.386-476 -GTG-AACCAG-C-TCGGGGGGG-TG-TTT-GTGAACGGCCGGCCC-TACCC-GAC
   F05WJXW02HXO3R.376-502 -GTG-AACCAG-C-TCGGGGGGG-TG-TT-GGTGAACGGCCGGCCCCTACC--GAC
   F05WJXW02IMYAO.376-523 -GTG-AACCAG-C-TCGGGGGGG-TG-TTT-GTGAACGGCCGGCCCCTACCC-GAC
     F05WJXW02GH4Q3.141-1 -GTG-AACCAG-C-TCGGGGGGG-TG-TTT-GTGAACGGCCGGCCCCTACCC-GAC
     F05WJXW02GM7GR.154-1 -GTG-AACCAG-C-TCGGGGGGG-TG-TTT-GTGAACGGCCGGCCCCTACCC-GAC
     F05WJXW02HHXPI.150-1 -GTG-AACCAG-C-TCGGGGGGG-TG-TT-CGTGAACGGCCGGCCCCTACCC-GAC
     F05WJXW02GEKNF.159-1 -GTG-AACCAG-C-TCGGGGGGG-TG-TTTTGTGAACGGCCGGCCCCTACCC-GAC
   F05WJXW02JD7QE.351-458 -GTG-AACCAG-C-TCGGGGGGG-TG-TTT-GTGAACGGCCGGCCC-TACCC-GAC
     F05WJXW02F2STE.150-1 -GTG-AACCAG-C-TCGGGGGGG-TG-TTT-GTGAACGGCCGGCCCCTACCC-GAC
   F05WJXW02I9BG2.344-532 -NTG-AACCAG-C-TCGGGGGGGGTN-TTT-GTGGACGGCCGGCCCCTACCC-GAC
   F05WJXW02IGCSO.343-523 -GTG-AACCAG-C-TCGGGGGGGGTG-TTTGGTGAACGGCCGGCCCCTACCC-GAC
     F05WJXW02HWDHW.202-1 -GTG-AACCAG-C-TCGGGGGGG-TG-TTT-GTGAACGGCCGGCCCCTACCC-GAC
   F05WJXW02GNODJ.327-434 -GTG-AACCAG-C-TCGGGGGGGGTG-TTT-GTGAACGGCCGGCCCCTACCC-GAC
   F05WJXW02JDH3C.325-460 -GTG-AACCAG-C-TCGGGGGGG-TG-TTT-GTGAACGGCCGGCCCCTACCC-GAC
     F05WJXW02FJQSP.157-1 -GTG-AACCAG-C-TCGGGGGGG-TG-TTT-GTGAACGGCCGGCCCCTACCC-GAC
     F05WJXW02JEI0H.208-4 -GTG-AACCAG-C-TCGGGGGGGGTG-TTT-GTGAACGGC-GGCCCCTACCCCGAC
     F05WJXW02GVKCB.147-1 -GTG-AACCAG-C-TCGGGGGGGGTG-TTTTGTGAACGGCCGGCCCCTACCC-GAC
     F05WJXW02HMWOV.121-1 -GTG-AACCAG-C-TCGGGGGGG-TG-TTT-GTGAACGGCCGGCCCCTACCC-GAC
     F05WJXW02G5EPO.191-1 -GTG-AACCAG-C-TCGGGGGGG-TG-TTT-GTGAACGGCCGGCCCCTACCC-GAC
```

Fig. 3. A screenshot from the CLCbio analysis software showing the frameshift mutation c.del77G. The mutated base is shown between the two vertical grey lines. The reads showing the mutant allele (6 Gs) are grouped at the top, while the reads generated from the wild-type allele (7 Gs) are shown at the bottom.

examples illustrate that appropriate evaluation of detected changes in patient specimens will often require parental testing and functional analysis. This requirement may represent a significant challenge in the clinical settings.

Multiple known single-nucleotide polymorphisms were detected, providing reassurance that both SCE and GS FLX sequencing performed as expected. For example, Sample 2 showed presence of the previously described polymorphism in the exon 8 of the *PAX2* gene 1521A > C, P326P (rs1800898) [38].

Discussion

SCE and GS FLX sequencing allowed us to simultaneously sequence 112 candidate genes for ocular birth defects in two independent DNA samples, and to detect two known mutations in the *PAX2* gene.

Although whole genome sequencing represents the most comprehensive approach to identifying disease causing mutations in patients with hereditary disorders, such sequencing and analysis is not yet possible [39]. We therefore focused our studies on genes which are known to be associated with ocular birth defects, as well as numerous candidate genes which play a role in regulating early eye development.

To overcome the limitations of target enrichment by PCR, we used high-density SCE microarrays for selecting and capturing relevant exons [29–32]. The GS FLX instrument with Titanium chemistry was chosen based on its ability to produce long reads which are advantageous for sequencing complex genomes. Additionally, protocols for target enrichment by array based SCE were originally developed and optimized for the GS FLX system. However, our methods can be easily adapted for use with other sequencing platforms, like the Genome Analyzer IIx from Illumina (Illumina, Inc., San Diego, CA) and the SOLiD System from Applied Biosystems (Life Technologies, Carlsbad, CA).

In our pilot study "hands on" and instrument run times for sequencing 112 genes in two independent specimens were measured in days, while the cost was less than $8000 per sample ($3000 for SCE and ~$5000 for sequencing). Performing enrichment by traditional PCR and Sanger sequencing for the same number of genes would have been a daunting task, even for facilities with high levels of automation and high throughput. Although our costs for performing SCE and NGS were high compared to savings that can potentially be achieved with these technologies, they were still modest since the price for diagnostic Sanger sequencing for only one gene can be thousands of dollars. Furthermore, there are multiple ways to further optimize our approach. Significant increase in sequencing quality and throughput and decrease in cost can be achieved by: (1) running multiple samples in the same run either by separating them physically (with gaskets) or by adding short oligonucleotide adapters as "barcodes", and running the samples as a pool [40,41], (2) optimizing the custom SCE array to achieve more uniform coverage, by adding additional probes for poorly performing regions and (3) using improved SCE protocols which require smaller amounts of DNA sample and allow adding GS FLX sequencing linkers during the SCE stage [42].

Since the capacity of the 385,000 probe array is higher than our current targeted region, it will be feasible to expand our project by adding new genes as they are implicated in ocular birth defects. In addition, we may perform further studies to compare the microarray capture method with solution phase based enrichment methods, such as Agilent's SureSelect.

GS FLX sequencing clearly identified the known missense mutation in our Sample 1, but was less successful in detecting the one base deletion in a long homonucleotide stretch, that had previously been identified by Sanger sequencing. Homonucelotide stretches are particularly problematic to accurately analyze using the pyrosequencing based GS FLX system, as demonstrated by identification of alterations in the numbers of homonucleotides that could not be confirmed by Sanger sequencing. Since homonucleotide repeats represent hotspots for disease causing mutations in humans, accurate detection of insertions and deletions in these regions is very important for the use of NGS in the clinical setting, and will require further optimization. For the GS FLX system, the problem may be solvable by better analysis algorithms or manual review as well as Sanger sequencing confirmation for regions containing >6 copies of the same base. Alternatively, users may consider SOLiD or Illumina instruments, which are based on other chemistries and have a different error profile.

Current concerns in application of SCE–NGS methods for mutation analysis in research and clinical settings include (1) lack of definitive parameters for distinguishing false positives (sequencing errors) from real sequence changes, (2) insufficient information about false negative rate, (3) lack of guidelines for dealing with the overwhelming number of detected sequence variants, (4) systematic technical artifacts due to duplicated sequences in the genome (large gene families, pseudogenes etc.), (5) decreased ability to detect gene interruptions due to insertions of Alu repeats and other repetitive sequences [12], (6) storage and management of massive amounts of data and (7) reporting and ethical considerations.

False positive and false negative rates are vital for clinical applications of NGS, and are known to significantly depend on the level of sequencing coverage. Smith et al. [36] have shown that ∼15-fold redundant coverage allows accurate mutational profiling in haploid organisms, while deeper coverage should be applied for diploid genomes (we used 30× coverage as a threshold in our study). However, there are currently no recommendations regarding the minimum percentage of reads which should show a variant allele in order to confidently establish a heterozygous allele call (we applied an arbitrary cut-off of 30%).

Approaches that are typically used in NGS to filter huge numbers of detected (real) variants and distinguish clinically relevant changes from benign polymorphisms include (1) comparing detected changes with public databases of known sequence variants (dbSNP) (2) considering only non-synonymous sequence changes and (3) analyzing by PolyPhen or SIFT whether a change is likely to be damaging for the function of the encoded protein. Comparison with public databases is likely to become even more helpful in the future, when the 1000 Genomes Project [43] generates a catalogue of common variation that is more complete and more evenly ascertained than dbSNP.

Interference from homologous sequences (pseudogenes, members of the same gene family) may result in false positives due to mismapped reads from duplicated regions with related sequences. This problem is ameliorated by removal of reads with non-unique placements during read alignment. However, this decreases sensitivity for detecting mutations, making it difficult to reliably test genes which have paralogs with highly identical sequences.

Table 3
Non-synonymous coding sequence changes detected in Samples 1 and 2, which do not correspond to known SNPs.

Chromosome	Reference position	Gene name	Coverage depth	Reference nucleotide	Variant nucleotide	Variant percentage (%)	Reference AA	Variant AA	Homo-nucleotide	Sanger sequencing result	PolyPhen prediction	SIFT prediction
Sample 1												
chr10	123,235,026	*FGFR2*	99	CGA	Deletion	32	FG	PX (frameshift)	YES (four Cs)	Not confirmed		
chr2	169,746,208	*LRP2*	168	T	C	52	I	V	–	Confirmed	Possibly damaging	Tolerated
chr2	144,872,994	*ZEB2*	150	T	C	46	I	V	–	Confirmed	Benign	Tolerated
chr2	135,642,699	*RAB3GAP1*	158	C	T	49	R	C	–	Confirmed	Probably damaging	Affects protein function
chr15	91,356,594	*CHD2*	146	T	Deletion	37	F	X (frameshift)	YES (five Ts)	Not confirmed		
Sample 2												
chr5	112,202,576	*APC*	188	T	C	49	L	S	–	Confirmed	Benign	Affects protein function (low confidence prediction)[a]
chr5	112,203,856	*APC*	148	A	Deletion	37	T	X (frameshift)[*]	YES (six As)	Not confirmed		
chr2	169,750,453	*LRP2*	155	A	Deletion	36	Y	X (frameshift)	YES (four As)	Not confirmed		

[a] This SIFT prediction was described as "low confidence". The amino-acid change may have been predicted to affect the protein function just because other protein sequences used for comparison were not diverse enough.

Data storage and analysis are large challenges for individual laboratories considering use of NGS. The issue of data storage is further complicated by the consideration of how much of the dataset to keep (image data, raw data or just fasta files). The bioinformatics challenges are alleviated by core facilities offering data retention on their servers, access to analysis software and consultation with bioinformatics experts. Additionally, it has been proposed that cloud-computing solutions which provide internet access to large clusters of computers may allow investigators from small laboratories to access data analysis tools and significant hardware power at a reasonable cost [44].

Large sample sets will need to be studied and specific, objective, evidence based guidelines and quality controls developed to address main technical issues and enable use of SCE and NGS technologies to reliably detect pathogenic mutations in research and diagnostics laboratories. Routine Sanger sequencing will likely be required for a long time to confirm data generated by NGS. Even when technical limitations get resolved, serious test reporting issues and ethical considerations are likely to remain. For example, each person is likely to carry multiple clinically relevant mutations which can be detected by genome-wide sequencing. It is unclear should participants in NGS based studies receive all their sequencing information (even when it is not possible to implement effective medical treatments for clinically relevant variants) and how should this information be delivered and interpreted to patients [45].

In conclusion, our study showed that even with existing limitations, individual researchers working with core sequencing facilities can use NGS as a research tool with confidence and ease. In the near future, thanks to continuing improvements in throughput, accuracy, cost and ease of data analysis, it will also become feasible to apply NGS in the clinical setting.

Acknowledgments

We gratefully acknowledge Einat Snir and Jennifer Bair from The University of Iowa DNA Facility for technical assistance with GS FLX sequencing and manuscript review, and Eric Cabot from the University of Wisconsin-Madison Biotechnology Center for help with reviewing the sequencing data.

References

[1] J.R. ten Bosch, W.W. Grody, Keeping up with the next generation: massively parallel sequencing in clinical diagnostics, J. Mol. Diagn. 10 (2008) 484–492.

[2] K.V. Voelkerding, S.A. Dames, J.D. Durtschi, Next-generation sequencing: from basic research to diagnostics, Clin. Chem. 55 (2009) 641–658.

[3] T. Tucker, M. Marra, J.M. Friedman, Massively parallel sequencing: the next big thing in genetic medicine, Am. J. Hum. Genet. 85 (2009) 142–154.

[4] S.C. Schuster, Next-generation sequencing transforms today's biology, Nat. Methods 5 (2008) 16–18.

[5] S. Marguerat, B.T. Wilhelm, J. Bahler, Next-generation sequencing: applications beyond genomes, Biochem. Soc. Trans. 36 (2008) 1091–1096.

[6] H.H. Ropers, Genetics of intellectual disability, Curr. Opin. Genet. Dev. 18 (2008) 241–250.

[7] W.E. Nance, The genetics of deafness, Ment. Retard. Dev. Disabil. Res. Rev. 9 (2003) 109–119.

[8] A.J. Marian, Genetic determinants of cardiac hypertrophy, Curr. Opin. Cardiol. 23 (2008) 199–205.

[9] P. Goodwin, Hereditary retinal disease, Curr. Opin. Ophthalmol. 19 (2008) 255–262.

[10] C. Gabriel, M. Danzer, C. Hackl, G. Kopal, P. Hufnagl, K. Hofer, H. Polin, S. Stabentheiner, J. Proll, Rapid high-throughput human leukocyte antigen typing by massively parallel pyrosequencing for high-resolution allele identification, Hum. Immunol. 70 (2009) 960–964.

[11] G. Bentley, R. Higuchi, B. Hoglund, D. Goodridge, D. Sayer, E.A. Trachtenberg, H.A. Erlich, High-resolution, high-throughput HLA genotyping by next-generation sequencing, Tissue Antigens 74 (2009) 393–403.

[12] L.S. Chou, C.S. Liu, B. Boese, X. Zhang, R. Mao, DNA sequence capture and enrichment by microarray followed by next-generation sequencing for targeted resequencing: neurofibromatosis type 1 gene as a model, Clin. Chem. 56 (2010) 1–11.

[13] A. Hoischen, C. Gilissen, P. Arts, N. Wieskamp, W. van der Vliet, S. Vermeer, M. Steehouwer, P. de Vries, R. Meijer, J. Seiqueros, N.V.A.M. Knoers, M.F. Buckley, H. Scheffer, J.A. Veltman, Massively parallel sequencing of ataxia genes after array-based enrichment, Hum. Mutat., doi:10.1002/humu.21221 (Published on-line 11 Feb 2010).

[14] V. Vasta, S.B. Ng, E.H. Turner, J. Shendure, S.H. Hahn, Next generation sequence analysis for mitochondrial disorders, Genome Med. 1 (2009) 100.

[15] S.B. Ng, E.H. Turner, P.D. Robertson, S.D. Flygare, A.W. Bigham, C. Lee, T. Shaffer, M. Wong, A. Bhattacharjee, E.E. Eichler, M. Bamshad, D.A. Nickerson, J. Shendure, Targeted capture and massively parallel sequencing of 12 human exomes, Nature 461 (2009) 272–276.

[16] S.B. Ng, K.J. Buckingham, C. Lee, A.W. Bigham, H.K. Tabor, K.M. Dent, C.D. Huff, P.T. Shannon, E.W. Jabs, D.A. Nickerson, J. Shendure, M.J. Bamshad, Exome sequencing identifies the cause of a Mendelian disorder, Nat. Genet. 42 (2010) 30–35.

[17] T.J. Ley, E.R. Mardis, L. Ding, B. Fulton, M.D. McLellan, K. Chen, D. Dooling, B.H. Dunford-Shore, S. McGrath, M. Hickenbotham, L. Cook, R. Abbott, D.E. Larson, D.C. Koboldt, C. Pohl, S. Smith, A. Hawkins, S. Abbott, D. Locke, L.W. Hillier, T. Miner, L. Fulton, V. Magrini, T. Wylie, J. Glasscock, J. Conyers, N. Sander, X. Shi, J.R. Osborne, P. Minx, D. Gordon, A. Chinwalla, Y. Zhao, R.E. Ries, J.E. Payton, P. Westervelt, M.H. Tomasson, M. Watson, J. Baty, J. Ivanovich, S. Heath, W.D. Shannon, R. Nagarajan, M.J. Walter, D.C. Link, T.A. Graubert, J.F. DiPersio, R.K. Wilson, DNA sequencing of a cytogenetically normal acute myeloid leukaemia genome, Nature 456 (2008) 66–72.

[18] E.R. Mardis, L. Ding, D.J. Dooling, D.E. Larson, M.D. McLellan, K. Chen, D.C. Koboldt, R.S. Fulton, K.D. Delehaunty, S.D. McGrath, L.A. Fulton, D.P. Locke, V.J. Magrini, R.M. Abbott, T.L. Vickery, J.S. Reed, J.S. Robinson, T. Wylie, S.M. Smith, L. Carmichael, J.M. Eldred, C.C. Harris, J. Walker, J.B. Peck, F. Du, A.F. Dukes, G.E. Sanderson, A.M. Brummett, E. Clark, J.F. McMichael, R.J. Meyer, J.K. Schindler, C.S. Pohl, J.W. Wallis, X. Shi, L. Lin, H. Schmidt, Y. Tang, C. Haipek, M.E. Wiechert, J.V. Ivy, J. Kalicki, G. Elliott, R.E. Ries, J.E. Payton, P. Westervelt, M.H. Tomasson, M.A. Watson, J. Baty, S. Heath, W.D. Shannon, R. Nagarajan, D.C. Link, M.J. Walter, T.A. Graubert, J.F. DiPersio, R.K. Wilson, T.J. Ley, Recurring mutations found by sequencing an acute myeloid leukemia genome, N. Engl. J. Med. 361 (2009) 1058–1066.

[19] D.W. Parsons, S. Jones, X. Zhang, J.C. Lin, R.J. Leary, P. Angenendt, P. Mankoo, H. Carter, I.M. Siu, G.L. Gallia, A. Olivi, R. McLendon, B.A. Rasheed, S. Keir, T. Nikolskaya, Y. Nikolsky, D.A. Busam, H. Tekleab, L.A. Diaz Jr., J. Hartigan, D.R. Smith, R.L. Strausberg, S.K. Marie, S.M. Shinjo, H. Yan, G.J. Riggins, D.D. Bigner, R. Karchin, N. Papadopoulos, G. Parmigiani, B. Vogelstein, V.E. Velculescu, K.W. Kinzler, An integrated genomic analysis of human glioblastoma multiforme, Science 321 (2008) 1807–1812.

[20] E.R. Mardis, R.K. Wilson, Cancer genome sequencing: a review, Hum. Mol. Genet. 18 (2009) R163–R168.

[21] C. Stoll, Y. Alembik, B. Dott, M.P. Roth, Congenital eye malformations in 212,479 consecutive births, Ann. Genet. 40 (1997) 122–128.

[22] J.R. Guercio, L.J. Martyn, Congenital malformations of the eye and orbit, Otolaryngol. Clin. North Am. 40 (2007) 113–140. vii.

[23] C.Y. Gregory-Evans, M.J. Williams, S. Halford, K. Gregory-Evans, Ocular coloboma: a reassessment in the age of molecular neuroscience, J. Med. Genet. 41 (2004) 881–891.

[24] D.R. Fitzpatrick, V. van Heyningen, Developmental eye disorders, Curr. Opin. Genet. Dev. 15 (2005) 348–353.

[25] L. Chang, D. Blain, S. Bertuzzi, B.P. Brooks, Uveal coloboma: clinical and basic science update, Curr. Opin. Ophthalmol. (2006) 447–470.

[26] L.A. Schimmenti, H.H. Shim, J.D. Wirtschafter, V.A. Panzarino, C.E. Kashtan, S.J. Kirkpatrick, D.S. Wargowski, T.D. France, E. Michel, W.B. Dobyns, Homonucleotide expansion and contraction mutations of PAX2 and inclusion of Chiari 1 malformation as part of renal-coloboma syndrome, Hum. Mutat. 14 (1999) 369–376.

[27] J.M. Gross, B.D. Perkins, Zebrafish mutants as models for congenital ocular disorders in humans, Mol. Reprod. Dev. 75 (2008) 547–555.

[28] C. Alescaron, R.T. Ernst, Anterior eye development and ocular mesenchyme: new insights from mouse models and human diseases, Bioessays 26 (2004) 374–386.

[29] Roche-NimbleGen Inc, Roche Nimble-Gen probe design fundamentals. Application Notes. Available from: <http://www.nimblegen.com/products/lit/probe_design_2008_06_04.pdf> (accessed December 2009).

[30] Roche-NimbleGen Inc, NimbleGen services user's guides: sequence capture service. Application Notes. Available from: <http://www.nimblegen.com/products/lit/SeqCap_UsersGuide_Service_v3p0.pdf> (accessed December 2009).

[31] M. Olson, Enrichment of super-sized resequencing targets from the human genome, Nat. Methods 4 (2007) 891–892.

[32] T.J. Albert, M.N. Molla, D.M. Muzny, L. Nazareth, D. Wheeler, X. Song, T.A. Richmond, C.M. Middle, M.J. Rodesch, C.J. Packard, G.M. Weinstock, R.A. Gibbs, Direct selection of human genomic loci by microarray hybridization, Nat. Methods 4 (2007) 903–905.

[33] M. Margulies, M. Egholm, W.E. Altman, S. Attiya, J.S. Bader, L.A. Bemben, J. Berka, M.S. Braverman, Y.J. Chen, Z. Chen, S.B. Dewell, L. Du, J.M. Fierro, X.V. Gomes, B.C. Godwin, W. He, S. Helgesen, C.H. Ho, G.P. Irzyk, S.C. Jando, M.L. Alenquer, T.P. Jarvie, K.B. Jirage, J.B. Kim, J.R. Knight, J.R. Lanza, J.H. Leamon, S.M. Lefkowitz, M. Lei, J. Li, K.L. Lohman, H. Lu, V.B. Makhijani, K.E. McDade, M.P. McKenna, E.W. Myers, E. Nickerson, J.R. Nobile, R. Plant, B.P. Puc, M.T. Ronan, G.T. Roth, G.J. Sarkis, J.F. Simons, J.W. Simpson, M. Srinivasan, K.R. Tartaro, A. Tomasz, K.A. Vogt, G.A. Volkmer, S.H. Wang, Y. Wang, M.P. Weiner,

P. Yu, R.F. Begley, J.M. Rothberg, Genome sequencing in microfabricated high-density picolitre reactors, Nature 437 (2005) 376–380.

[34] J.M. Rothberg, J.H. Leamon, The development and impact of 454 sequencing, Nat. Biotechnol. 26 (2008) 1117–1124.

[35] E.R. Mardis, Next-generation DNA sequencing methods, Annu. Rev. Genomics Hum. Genet. 9 (2008) 387–402.

[36] D.R. Smith, A.R. Quinlan, H.E. Peckham, K. Makowsky, W. Tao, B. Woolf, L. Shen, W.F. Donahue, N. Tusneem, M.P. Stromberg, D.A. Stewart, L. Zhang, S.S. Ranade, J.B. Warner, C.C. Lee, B.E. Coleman, Z. Zhang, S.F. McLaughlin, J.A. Malek, J.M. Sorenson, A.P. Blanchard, J. Chapman, D. Hillman, F. Chen, D.S. Rokhsar, K.J. McKernan, T.W. Jeffries, G.T. Marth, P.M. Richardson, Rapid whole-genome mutational profiling using next-generation sequencing technologies, Genome Res. 18 (2008) 1638–1642.

[37] T. Wicker, E. Schlagenhauf, A. Graner, T.J. Close, B. Keller, N. Stein, 454 sequencing put to the test using the complex genome of barley, BMC Genomics 7 (2006) 275.

[38] H.H. Shim, B.N. Nakamura, R.M. Cantor, L.A. Schimmenti, Identification of two single nucleotide polymorphisms in exon 8 of PAX2, Mol. Genet. Metab. 68 (1999) 507–510.

[39] D. Summerer, Enabling technologies of genomic-scale sequence enrichment for targeted high-throughput sequencing, Genomics 94 (2009) 363–368.

[40] M. Meyer, U. Stenzel, S. Myles, K. Prufer, M. Hofreiter, Targeted high-throughput sequencing of tagged nucleic acid samples, Nucleic Acids Res. 35 (2007) e97.

[41] M. Meyer, U. Stenzel, M. Hofreiter, Parallel tagged sequencing on the 454 platform, Nat. Protoc. 3 (2008) 267–278.

[42] Roche-NimbleGen Inc., NimbleGen titanium optimized sequence capture 385 K arrays. Application Notes. Available from: <http://www.454.com/downloads/products-solutions/SeqCapTitan385K_Final.pdf> (accessed December 2009).

[43] N. Siva, 1000 genomes project, Nat. Biotechnol. 26 (2008) 256.

[44] J.D. McPherson, Next-generation gap, Nat. Methods 6 (2009) S2–S5.

[45] L.G. Biesecker, Exome sequencing makes medical genomics a reality, Nat. Genet. 42 (2010) 13–14.